Food Bioprocess Technol
DOI 10.1007/s11947-008-0167-6

ORIGINAL PAPER

A Systematic Approach for Solving Large-Scale Problems by Neural Network: Open Refrigerated Display Cases and Droplet Evaporation Problems

Mazyar Amin · Homayun K. Navaz · Nasser Kehtarnavaz · Dana Dabiri

Received: 31 December 2007 / Accepted: 19 November 2008

Abstract A systematic approach for solving a large-scale design problem is proposed. The method consists of building a multidimensional test case matrix connecting an output (scalar or vector) to an input vector. Every element of the input vector spans over its possible minimum and maximum values with one or more levels in between. The experimental and validated computational methods are combined to find the output as a function of all permutations of the input variables. The results are used to train a neural network program to perform the proper interpolation for any other expected scenario. The number of required experiments is obtained asymptotically by adding more data to the neural network training set and examining the error. The applicability and feasibility of this approach is shown in two different problems: first, predicting and minimizing the infiltration rate into an open refrigerated display case; and second, predicting the evaporation rate of sessile microdroplets on a nonpermeable surface.

Keywords Neural network · Large-scale problem · Infiltration rate · Refrigerated display case · Chemical agent fate

M. Amin (✉) · D. Dabiri
Aeronautics and Astronautics Department,
University of Washington,
Seattle, WA 98195, USA
e-mail: mazyar@u.washington.edu

H. K. Navaz
Mechanical Engineering Department, Kettering University,
Flint, MI 48504, USA

N. Kehtarnavaz
Electrical Engineering Department, University of Texas at Dallas,
Dallas, TX 75080, USA

Published online: 19 December 2008

Introduction

Many engineering problems have a high level of complexity due to certain parameters such as geometry, conditions of operation, and range of applicability. In the area of fluid flow, such parameters are introduced through geometrical variables, turbulence and flow structures, concentration and temperature gradients, pressure distributions, etc. The time and length scales may not necessarily coincide or be of the same order of magnitude for all phenomena present in a given problem adding further complexity to finding a solution. These flow problems are governed by the Navier–Stokes (NS) equations, and their numerical solutions have grown into an area of science and engineering called computational fluid dynamics (CFD). The Reynolds-averaged solution of the NS equations (RANS) requires physical models to be incorporated into the solution to these equations. Turbulence, viscosity (Newtonian vs. non-Newtonian), phase change, and chemical reaction kinetics are examples of physical models that need to accompany the NS equations to make the solution more practical and feasible.

Obtaining analytical/numerical solutions to complex fluid flow problems may be questionable if they are not verified with experimental results. This is mainly due to the existence of multiple solutions for the NS equations and also because the physical models are accompanying these equations. Obtaining a solution to NS equations only by conducting experiments is time consuming, may not be possible, or financially exhaustive. However, utilizing a numerical/computational technique such as a validated numerical solution will reduce the burden of excessive experimentations. Thus, a combined or hybrid approach provides a more feasible and realistic alternative. However, if the numbers of possible scenarios increase because of multitudinous permutations, a hybrid approach will also

become impractical. Consequently, creating an *engineering design tool* that can easily be used for parametric studies of a specific problem without the complexities of a fully hybrid approach is of great practical value. The goal of this study is to develop an artificial neural network (ANN) program to serve as the main tool.

Artificial neural network models were first introduced by McCulloch and Pitts in 1943, as was explained by Cheng and Titterington (1994). ANN models are algorithms that predict an outcome variable based on the values of some independent variables. A typical ANN model learns from examples and processes the information through special training algorithms that are developed based on learning rules (Hajmeer and Basheer 2003). The ANN will be developed to provide a practical tool to predict the outcome of a scenario that is defined by its input variables.

The ANN is a computer program that is capable of learning the patterns of the change of dependent variable(s) with respect to the independent variables via training samples. It resembles biological neural nets in two ways: (1) Knowledge is acquired through learning (training) processes, and (2) Knowledge is stored via interneuron connection strengths (weights).

ANN models consist of one input layer, at least one hidden layer, and one output layer of nodes. Figure 1 shows a typical ANN model with three layers. The first layer consists of n nodes for n independent variables $(x_0, \ldots, x_n)$, second layer (hidden layer) consists of m nodes, and finally, the output layer has r nodes for r outcome variables $(y_1, \ldots, y_r)$. The most commonly used ANN models are feed-forward back-propagation models (Fig. 1). In this type of model, every output variable (Y_k) is a function of all nodes in the hidden layer, and each node in the hidden layer is a function of input variables $(x_0, \ldots, x_n)$. No interaction is allowed between nodes of the same layer. The hidden layer (s) allows the model to handle the nonlinearity and complexity of the relationship of variables. An ANN model, similar to Fig. 1, will estimate an output vector $(\widehat{Y})$ as close as possible to the actual output vector (Y) by receiving an input signal vector X. The data will be processed in the hidden layer using each node's corresponding weight (w_{ji}), and then the processed data will be passed on to the output layer. An output vector of $\widehat{Y}$ will be estimated using each node's corresponding weight (v_{kj}). The numerical simulations can be performed off-line, and the results will be used to train the ANN program. The ANN will be a simple-to-use and extremely practical tool.

Artificial neural networks in fact provide an alternative paradigm or mechanism for performing regression or curve fitting as compared to classical regression methods. In other words, ANNs denote a tool that achieves an implementation of regression. The classical regression approaches are linear, whereas ANN is a generalization of regression to nonlinear systems. Many papers in various fields have used both regression and ANN for approximation applications. In essence, the main attribute of utilizing this alternative paradigm is that there is no need to assume an underlying distribution of data, and ANN can be applied to multivariate nonlinear problems. Furthermore, if the output data is spread over a wide range as input variables are altered, the clustering technique is attributed into the ANN to more accurately predict the outcome. The ANN resembles biological neural nets in two ways that were described previously.

It is the intention of this paper to demonstrate the feasibility and practicality of the proposed approach

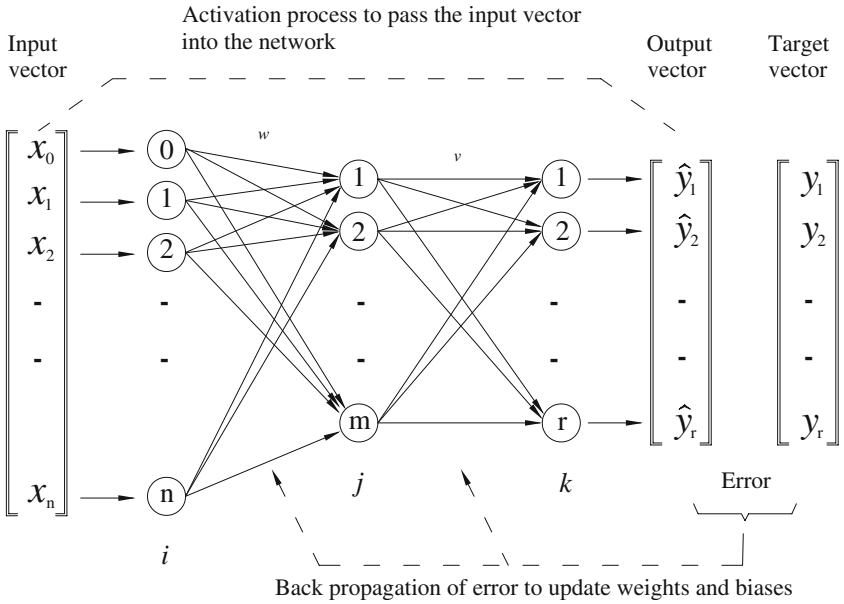

Fig. 1 Schematic of ANN model (Hajmeer and Basheer 2003)

through two entirely different examples. Both problems use their own corresponding input vector, but one has a scalar output, while the other has a functional output. We refer to this methodology as solution to large-scale engineering problems (SLEP).

While neural networks have been used to various capacities within food and bioprocess technologies, such as the work of Martins et al. (2008), Boyaci et al. (2008), and Patnaik (2008), the first part of our focus will be on the application of neural network towards solving large-scale problem in this industry. In this problem, the ANN is used as a tool to find the infiltration rate of warm air into a medium-temperature, open, refrigerated display case for any design configuration dictated by each manufacturer. The ANN can also be used to perform parametric studies for finding the specific input combination(s) that result in minimum infiltration rates. The second problem is transient evaporation of a sessile droplet on a nonpermeable surface subject to wind, i.e., convective evaporation. It is evident that the evaporation rate or the amount of remaining mass is a function of time; therefore, the ANN algorithm should be altered accordingly.

While the numerical solution of similar problems is computationally intensive and obtainable on supercomputers, they are of no practical value when a real-time response is necessary. The only practical solution is to perform the experiments and/or run the computer simulations for all the permutations of expected scenarios off-line and load the outputs into an ANN platform to enable proper prediction of unforeseen circumstances. Thus, the ANN will be "trained" based on the provided outcomes of certain events enabling it to make predictions of other possibilities. This prediction takes only seconds, making the ANN a more practical platform for field applications that can be run on any small computer.

Methods of Solution

Two large-scale problems are selected to demonstrate the accuracy and applicability of the ANN in providing an engineering tool with a fast turn-around time. One is a steady-state problem, and the other is a transient problem that requires an output as a function of time. The NN program is based on the ^{TM}LabView software and can be run on any system with Windows XP Operating System (Kehtarnavaz, N., User's Guide, LabVIEW-Based Neural Network Software).

Application of ANN to an Open Refrigerated Display Case—Steady State Problem

The first problem concerns open refrigerated display cases that are widely used in supermarkets to maintain the food products at prescribed temperatures. Cold air is provided through an inlet jet called the discharge air grille (DAG) located at the top front of the unit and through a group of slots located on the back panel of the case (see Fig. 2). The cold air jet at the top forms an invisible barrier between the outside warm air and the cold air inside the display case and enters the return air grille (RAG) located on the front and lower part of the display case. This invisible barrier is called the air curtain, and depending on its characteristics (velocity profile shape and magnitude, turbulence intensity, etc.) at the point of origin (i.e., the DAG), the curtain controls the amount of outside warm air that is pulled into the mixing zone. The continuous flow of warm air into the air curtain and its subsequent mixing with cold air is called entrainment. A portion of the entrained air spills over after some mixing with the cold air, and the rest is infiltrated into the RAG after it has increased the cold air temperature and thereafter imposes a cooling load on the refrigeration cycle. Obviously, the amount of infiltrated warm air should be kept to a minimum to conserve energy for running the cooling cycle to maintain a prescribed cold air temperature that is being driven to the DAG and the back panel. There have been numerous studies by Navaz et al. (2002, 2004, 2006a, b, 2007a) to identify parameters that can affect the infiltration rate in open refrigerated display cases. They have used a hybrid numerical and experimental approach to calculate the infiltration rate of the warm air into these display cases. Parameters that can significantly affect the air curtain characteristics are the Reynolds number at the DAG, the opening height, the offset distance (or angle) between the DAG and RAG, back panel flow ratio (to the total flow rate), and the throw angle (the angle of the exiting velocity vector at the DAG). Other parameters such as temperature, the amount of food products on the shelves, and the distribution of the back panel flow among the shelves can also alter the infiltration rate, though their impacts on the infiltration rates is less and of second-order effect. Therefore, by focusing on the most important parameters, we will show how the SLEP method can help engineers to improve their designs and also help manufacturers to know the infiltration rate of their current designs.

The infiltration rate within an open refrigerated display case can be directly measured by using carbon dioxide as a tracer gas. The equation relating the nondimensional infiltration rate (at the steady state) to the flow parameters is derived as (Amin et al. 2008):

$$\begin{aligned}\text{Non}-\text{Dimensional Infiltration} &= \left[\frac{(C_{CO_2})_{DAG}-(C_{CO_2})_{RAG}}{(C_{CO_2})_{DAG}-(C_{CO_2})_{Room}}\right] \\ &= f\left(\frac{H}{W_{DAG}}, \frac{\dot{m}_{BP}}{\dot{m}_{Total}}, Re, \alpha, \beta\right) \end{aligned} \quad (1)$$

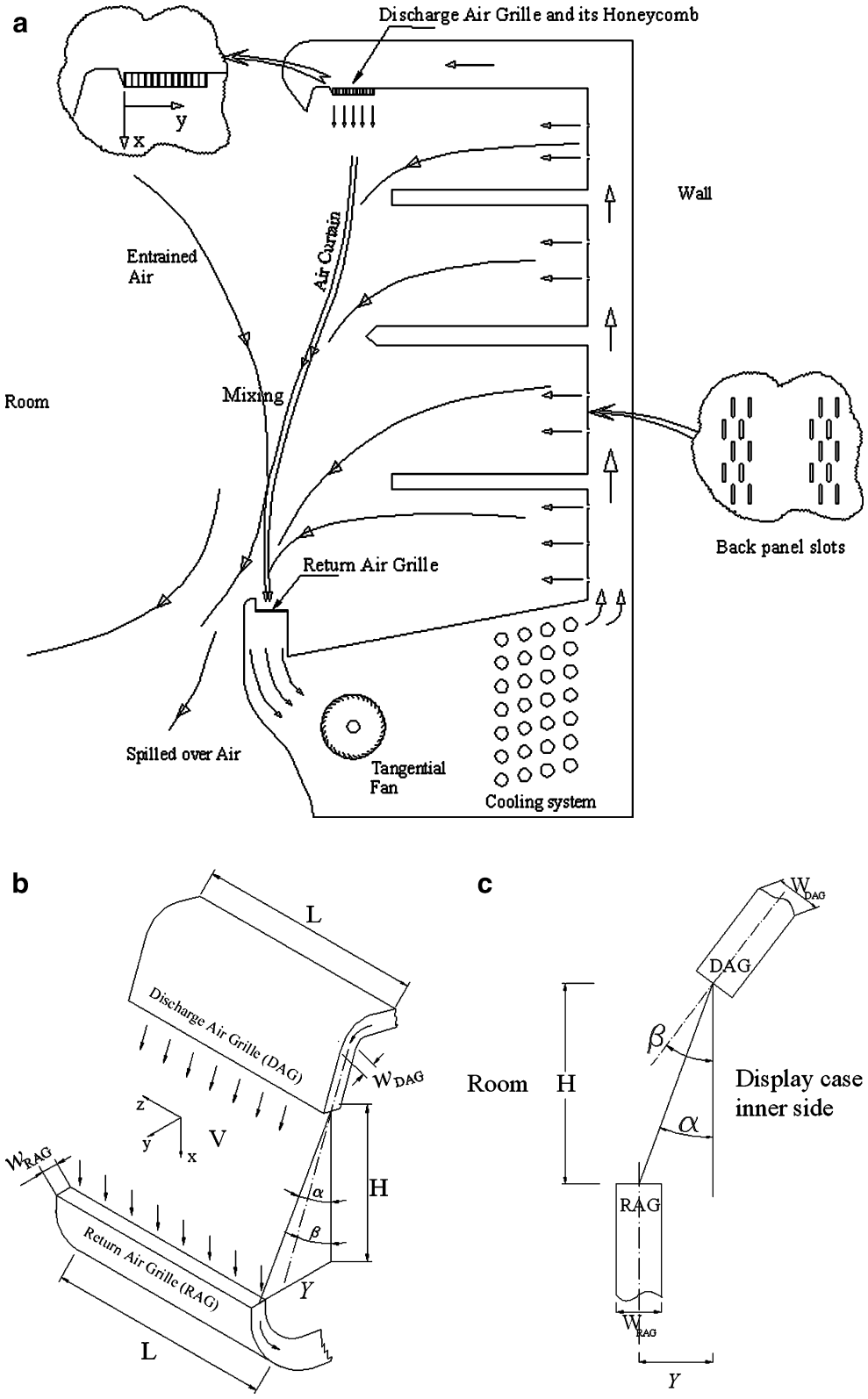

Fig. 2 Schematic of a typical open refrigerated display case with problem parameters

In this equation, C is the mass fraction of the tracer gas (CO_2 in this case), Re is the Reynolds number based on the DAG width, α is the offset angle, β is the throw angle, H is the vertical height of the opening, and $\frac{\dot{m}_{BP}}{\dot{m}_{Total}}$ represents the ratio of the back panel mass flow rate to the total display case mass flow rate. The mass flow rate can also be estimated with the volumetric flow rate if the density is maintained constant. The number of parameters can be increased without any impact on the methodology that is going to be discussed hereinafter.

A modular display case was designed and built as shown in Fig. 3. Sampling probes 1, 2, and 3 measure $(C_{CO2})_{DAG}$, $(C_{CO2})_{RAG}$, and $(C_{CO2})_{Room}$, respectively, which are used to calculate the nondimensional infiltration rate shown in Eq. 1. In this display case, it is possible to change all the problem variables (on the right side of Eq. 1), enabling us to measure the infiltration rate for all permutations (Navaz et al. 2005). A maximum and minimum "possible" value for each parameter is set. A certain number of levels between the maximum and minimum of each variable will specify the total number of permutations or experiments that need to be performed. In Table 1, the assumed maximum and minimum values and the number of levels for each variable are presented. It can be seen that, as the number of variables increases, the required number of experiments also increases significantly. Furthermore, as the number of levels increases, the number of infiltration rate measurements also grows considerably. The number of levels and the minimum/maximum for each variable was considered after numerous consultations with a team of experts and researchers from universities, organizations, and manufacturers. Initial CFD studies with the Fluent code demonstrated a monotonic variation of the infiltration rate as a function of H/W_{DAG} and α. However, the infiltration rate did not demonstrate the same behavior as a function of the Reynolds number or the throw angle and therefore required more values. These results were also verified with the experimental data and are addressed by Amin (2006) and Faramarzi et al. (2008). To cover the entire range of operation, a total number of 576 experiments should be performed. A hybrid approach that combines numerical and experimental results can be used to fill the permutation matrix. However, if the number of parameters and levels, which basically defines the matrix resolution, is increased simultaneously, the total number of required data points (numerical or experimental) will become prohibitively large.

Using an artificial neural network program provides a tool for interpolation of any unknown scenario from the provided known data points and allows for the reduction of the number of levels from the required data points. The importance of reducing the number of measurements can be appreciated when the usage of resources can be significantly reduced.

The process algorithm can be outlined:

Step 1: Assume the level of each variable (at least three levels to yield the minimum resolution for

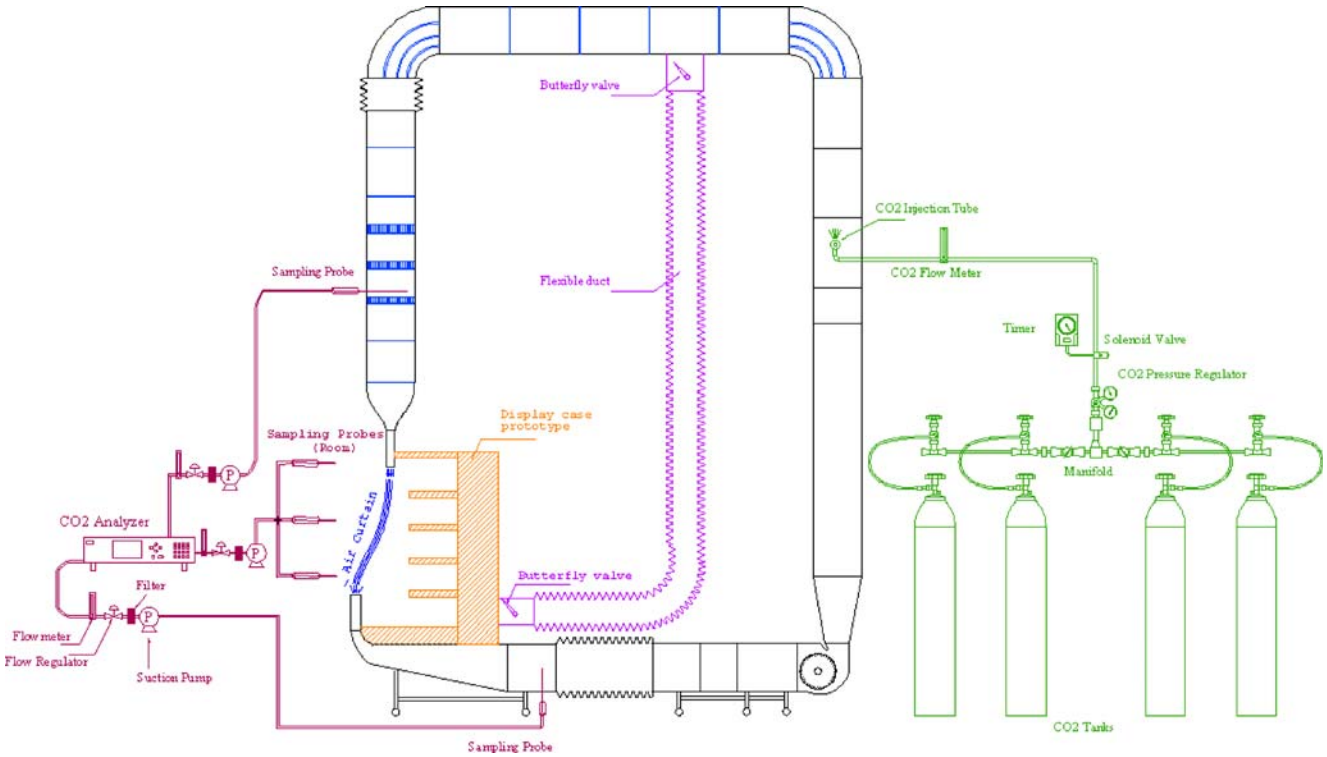

Fig. 3 Modular equipment setup

Table 1 Maximum, minimum, and number of levels for each variable

Variable	Minimum	Maximum	Levels	Number of Levels
H/W_{DAG}	8	16	8, 12, 16	3
$\dot{m}_{BP}/\dot{m}_{Total}$	0	1.0	Four levels (varies for different Reynolds numbers)	4
Re	2,000	8,400	2,200, 3,400, 5,500, 8,400	4
α	0°	24°	0°, 16°, 24°	3
β	−5°	13°	−5°, 0°, 5°, 13°	4

interpolation purposes) and randomly collect the infiltration data points. These points can be obtained by experimental or validated CFD programs.

Step 2: Train neural network program using 75% of these data.

Step 3: Validate several unknown scenarios (include mostly the remaining 25% of the data in step 1 that were not used in step 2) with the neural network tool and compare the results with the measured data, i.e., test the neural network prediction. It should be noted that these cases should be chosen randomly.

Step 4: If the results of step 3 are satisfactory, the prediction tool accuracy can be acceptable; if not, one additional level is added to the most sensitive variable, and steps 1 through 4 are repeated.

The test case matrix of the first problem is shown in Fig. 4. It contains different levels of the input (independent) variables appearing on the right-hand side of Eq. 1 and has 576 cells for the outputs (dependent variable). Each cell in the table represents the *nondimensional infiltration rate* data point at a specific permutation. For instance, the value of the hatched cell in Fig. 4 will correspond to a permutation at $(H/W_{DAG})_3$, $\left(\frac{\dot{m}_{BP}}{\dot{m}_{Total}}\right)_4$, Re_4, α_3, β_4. As stated in step 1, a number of test conditions are randomly selected; this number can be noticeably less than the total number of permutations. This selection will have to be made uniformly from the entire matrix. The randomly selected cells are marked by "X." The corresponding nondimensional infiltration rates of these cells are found by experimental and/or numerical models. The ANN program is *trained* by these data to obtain multidimensional functions. When the functions are available, the input conditions of a few cells marked by "X" will be fed into the neural network for *validation*. The output will be the predicted values of the cells, which ideally should be as close as possible to the actual values (computed or measured). If the difference between the predicted and the actual values is large, we increased the number of input data (experiments or marked cells). To implement this, a new series of random data marked with solid circles "•" (see Fig. 4) is added to the pool of "X" data. All the above steps taken for "X" cells should be repeated for a total of "X" and "•" cells. This procedure continues until the desired accuracy of the predictions is achieved.

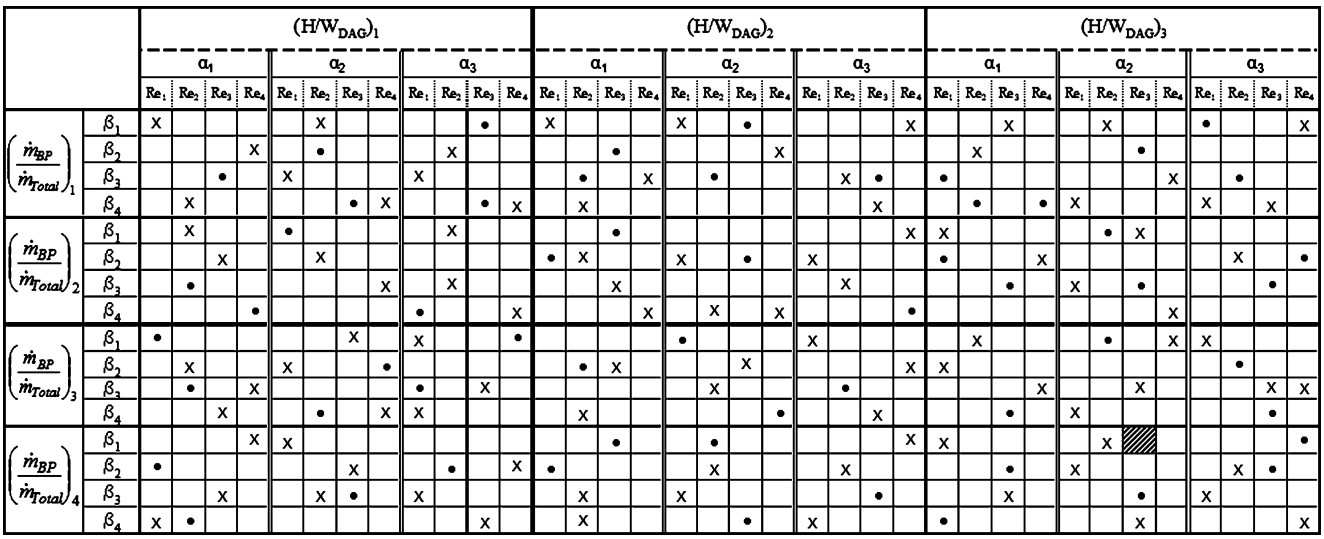

Fig. 4 Random selections of permutations in the test case matrix of first problem

Figure 5 shows the user interface of the NN training program. In the interface, in addition to feeding the input data files, some program parameters such as maximum number of epochs, step-sizes, etc. can be adjusted to produce more accurate outputs. Figure 6 is the recall interface that can be used for parametric studies as well as the prediction of infiltration rate for a specific design. In this interface, one can input the variables shown in Fig. 2. Then the normalized and absolute infiltration rates are calculated.

Based on the ANN results, it was predicted that, upon reducing the discharge grille velocity by about 25%, an 8% reduction in infiltration rate will be achieved. This value was verified by collecting water condensate and backing up the amount of fresh air that entered the display case over a 24-h period. The measured power saving during 24 h or the 24-h test indicated 6% reduction in kWh; the details can be found in Faramarzi et al. 2008.

Application of ANN to the Evaporation of a Sessile Droplet—Transient Problem

The second problem is chosen to demonstrate that the output can also be in the form of a function rather than a scalar number. There is a growing interest in predicting the fate of chemical agents after they are deposited onto a surface. The surface may be permeable or nonpermeable to a liquid agent. The process may be further complicated if there is a chemical reaction between the agent and the substrate. So far, there has not been any analytical model capable of predicting the amount of any chemical agent left in time given all the physical and chemical complexities that may occur between the agent and a porous substrate. The development of numerical methods capable of prediction of chemical agents' fates after they are deposited on porous or nonporous substrates is currently proceeding (Markicevic and Navaz 2007; Navaz et al. 2007b, 2007c, 2007d). The purpose of this test case is to predict the function that expresses the amount of normalized mass left during the evaporation as a function of time.

For the second problem, the evaporation rate has been shown to be a function of the friction velocity, air and droplet temperatures, droplet size, and number density deposited on the area as discussed by Navaz et al. (2006b, 2007b). It has been shown that embedded in the friction velocity is the free stream turbulence effects. It is evident that the amount of remaining mass is a function of time, which is represented by the evaporation rate. Therefore, an input vector results in an output that is a function (of time) rather than a single number.

We have chosen the modeling of convective evaporation of microdrops on nonpermeable and nonreacting surfaces to

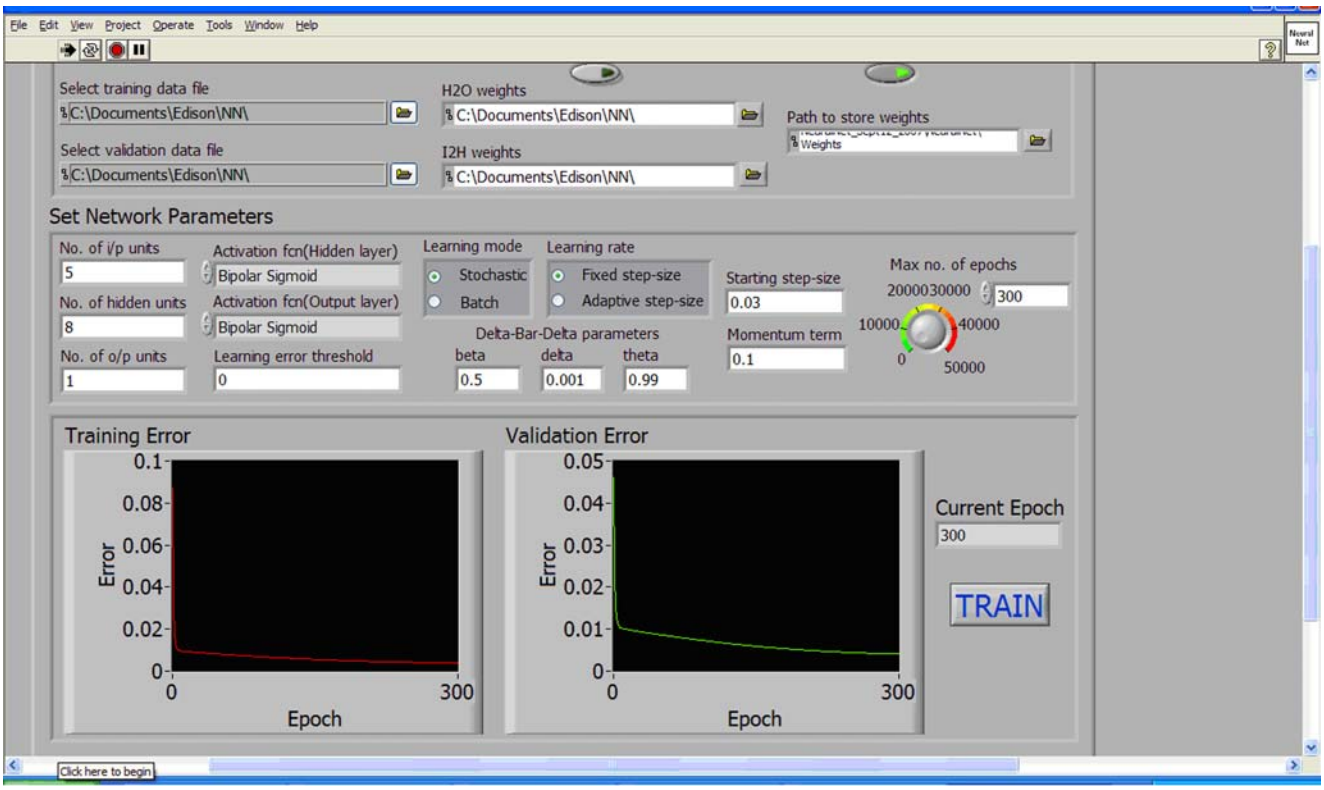

Fig. 5 The neural network training program user interface for the infiltration rate prediction

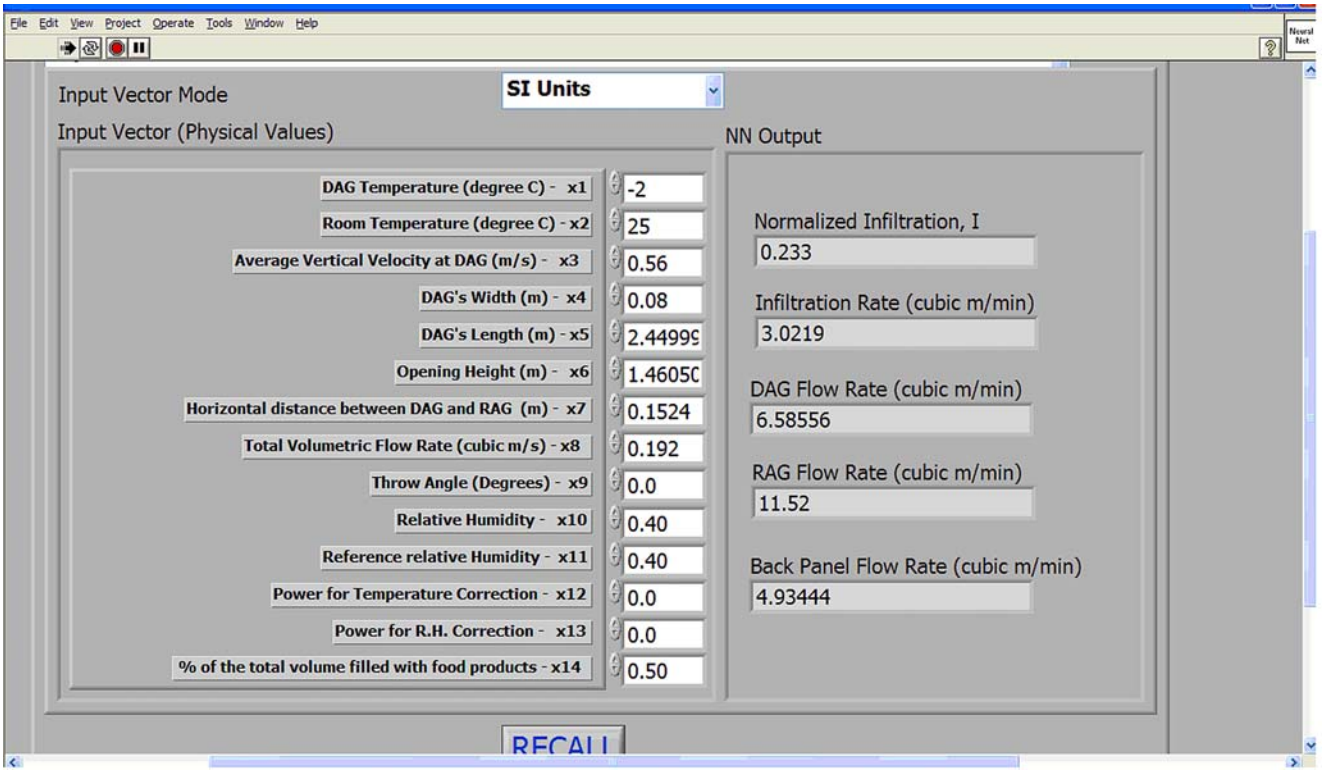

Fig. 6 The recall interface for the neural network prediction of infiltration rate

demonstrate the NN capabilities. Figure 7 shows a schematic of a sessile droplet in the form of a spherical cap residing on a nonpermeable surface subject to wind speed. As the evaporation occurs, the remaining mass will take the shape of a spherical cap. In this paper, we have used the chemical agent HD (known as Mustard agent) in its liquid form evaporating on a nonpermeable glass substrate.

The evaporation rate of a sessile drop on a nonpermeable/nonreacting substrate is derived by Navaz et al. (2006b, 2007b).

$$\dot{m}_{\text{evaporated}} = \frac{\mu}{Pr}\left(F_{\text{T}} + C_{\text{T}} Re^{m_{\text{T}}} Pr^{n_{\text{T}}}\right)\ell\text{n}[1 + \Lambda(T, Y_s)], \quad (2)$$

With:

$$\Lambda(T, Y_s) = \left(\frac{Y_s}{1 - Y_s}\right)^{\xi(\Theta)}$$

$$\text{where } \xi(\Theta) = -57.6148 + 174.5781\Theta - 172.7751\Theta^2 + 80.40564\Theta^3$$

$$\Theta = \frac{T}{T_{\text{ref}}}\,(\text{Absolute temperatures}) \text{ and } Y_s = \frac{P_{\text{vap}}}{P} \quad (3)$$

In these equations, $\dot{m}_{\text{evaporated}}$ is the mass flow rate, μ is the viscosity, Pr is the Prandtl number, $Re = \frac{\rho u^* R_s}{\mu}$ is the Reynolds number based on the droplet radius of curvature and friction velocity $u^* = \sqrt{\frac{\tau_w}{\rho}}$, with τ_w being the shear stress at the wall, P_{vap} is the vapor pressure, and F_{T}, m_{T}, n_T, and C_{T} are model constants obtained by wind tunnel experiments (Navaz et al. 2006b, 2007b). The natural log term represents the transfer or Spalding number. The free stream turbulence intensity alters the wall shear stress, and therefore, the use of the friction velocity will incorporate both the momentum and turbulence effects into the evaporation model as discussed in detail by Navaz et al.

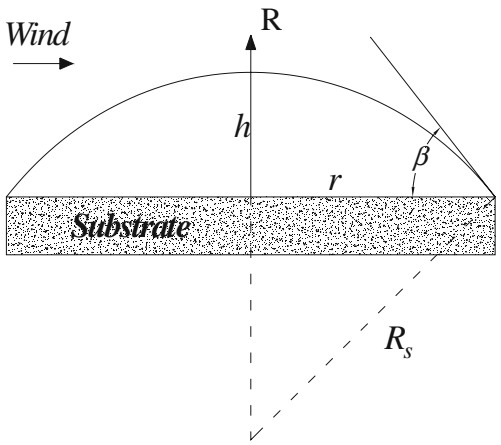

Fig. 7 Schematic of a sessile droplet on a substrate subject to wind conditions

Table 2 Minimum, maximum, and number of levels for the evaporation problem

Variable	Minimum	Maximum	Levels	Number of Levels
T_{air} (°C)	15	55	15, 25, 35, 50, 55	5
T_{drop} (°C)	15	55	15, 25, 35, 50, 55	5
u^* (m/s)	0.0285	0.1796	0.0285, 0.1038, 0.1534, 0.1796	4
V_{drop} (μL)	1	9	1, 6, 9	3
N_{drop}/Area (m^{-2})	3,600	10,000	3,600, 6,400, 10,000	3

(2007b). The instantaneous mass of the agent evaporating is obtained from Eq. 2 by the Runge–Kutta fourth-order numerical integration. The amount of normalized mass left can be calculated from the total evaporated mass as:

$$m_{left} = m_{initial} - \sum_{n=1}^{N} (n-1)\,\Delta t \frac{dm_{evaporated}}{dt}$$
$$\frac{m_{left}}{m_{initial}} = 1 - \frac{\sum_{n=1}^{N} (n-1)\,\Delta t \frac{dm_{evaporated}}{dt}}{m_{initial}} \quad (4)$$

It is known that for HD the initial contact angle on glass is about 32°. When evaporation starts, HD maintains the same base diameter, while the spherical cap is being reduced in height. When the contact angle reaches about 10°, the base diameter reduces, and the contact angle remains constant. Based on these observations and Eq. 4, the new topology of the droplet is found. We have used the model to provide the training set for the NN. Table 2 shows the variation of each parameter over the range of interest. The matrix that consists of all the permutations has 900 entries. The computer program was run for all 900 cases; however, the training set started with only 50 scenarios and was increased to 100 cases. The corner points and selected boundaries were intentionally included in the training set to bind the domain. The rest of the points were randomly selected by the ANN.

Results and Discussion

For the input variables shown in Eq. 1 or Table 1, the nondimensional infiltration rate of the outside air into the display case is considered to be the output. This quantity was measured initially for 150 different permutations, and the number was increased to about 250 and finally to 576. An additional 48 infiltration rates (not shown in Fig. 4) were experimentally measured for randomly selected values within the range from Fig. 4. The maximum training error under 1% for the ANN was observed. Therefore, it was concluded that the number of required tests has asymptotically reached an acceptable value well below the experimental error. Thus, this method attempts to asymptotically approach the optimum number of total data points (experimental, numerical, or hybrid) by progressively adding new series of data points to the existing input values of neural network. The 576 data points can sufficiently express the infiltration rate as

Table 3 Comparison of several actual and neural network nondimensional infiltration rate predictions

α (°)	β (°)	*Re*	$\dot{m}_{BP}/\dot{m}_{Total}$	*H/w*	Nondimensional infiltration rate		
					Actual	NN	% Error
0	−5	5,500	0	8	0.239	0.244	2.0
0	5	2,200	0.34	16	0.282	0.298	5.6
0	0	5,500	0.37	12	0.302	0.293	3.0
0	13	3,400	0.46	8	0.270	0.281	3.7
16	0	3,400	0.54	16	0.346	0.332	4.0
16	−5	8,400	0.41	16	0.295	0.320	8.0
16	13	8,400	0.41	8	0.329	0.314	4.6
16	5	5,500	0.37	16	0.376	0.392	4.2
24	−5	8,400	0	12	0.211	0.199	5.7
24	0	2,200	0.52	8	0.438	0.415	5.2
24	5	2,200	0.34	12	0.424	0.395	6.8
24	13	3,400	1	16	0.419	0.410	2.1

a function of all the variables. The trained neural network can be used as a design tool for parametric studies, where the input variables can be changed, and the infiltration rate will be calculated by the network within seconds.

Table 3 reflects some of the testing results of the neural network program. It should be mentioned that the NN comparison spans over the entire input domain. Figure 5 indicates that an error under 1% for the training is achieved. The ANN prediction for 50% of a randomly selected subset of 576 experiments was conducted. Table 3 just represents a short version of a large comparison. A maximum error of 8% was observed in the entire set, and this case is shown in Table 3. The coefficient of determination (R^2) was found to be about 0.945 for the whole pool of data (including the data used for training as well as validation), and as is evident, there is an excellent agreement between the ANN prediction and actual measurements as seen in Table 3.

In the second problem, a similar matrix as shown in Fig. 4 for this test case can be constructed with 900 possible scenarios. Conducting 900 experiments with dangerous agents could be very costly and is not a feasible option. Furthermore, the required 900 levels can easily be increased to several millions for more complex problems. It was found that the training of the ANN yielded sufficiently accurate results with a maximum error of 9% using only about 11% of the 900 data points (100 entries). The initial training was started with only 50 data points that yielded a maximum average error of 20%. The number of training sets was increased to 100 to lower the maximum average error. Figure 8a shows the error obtained during the training

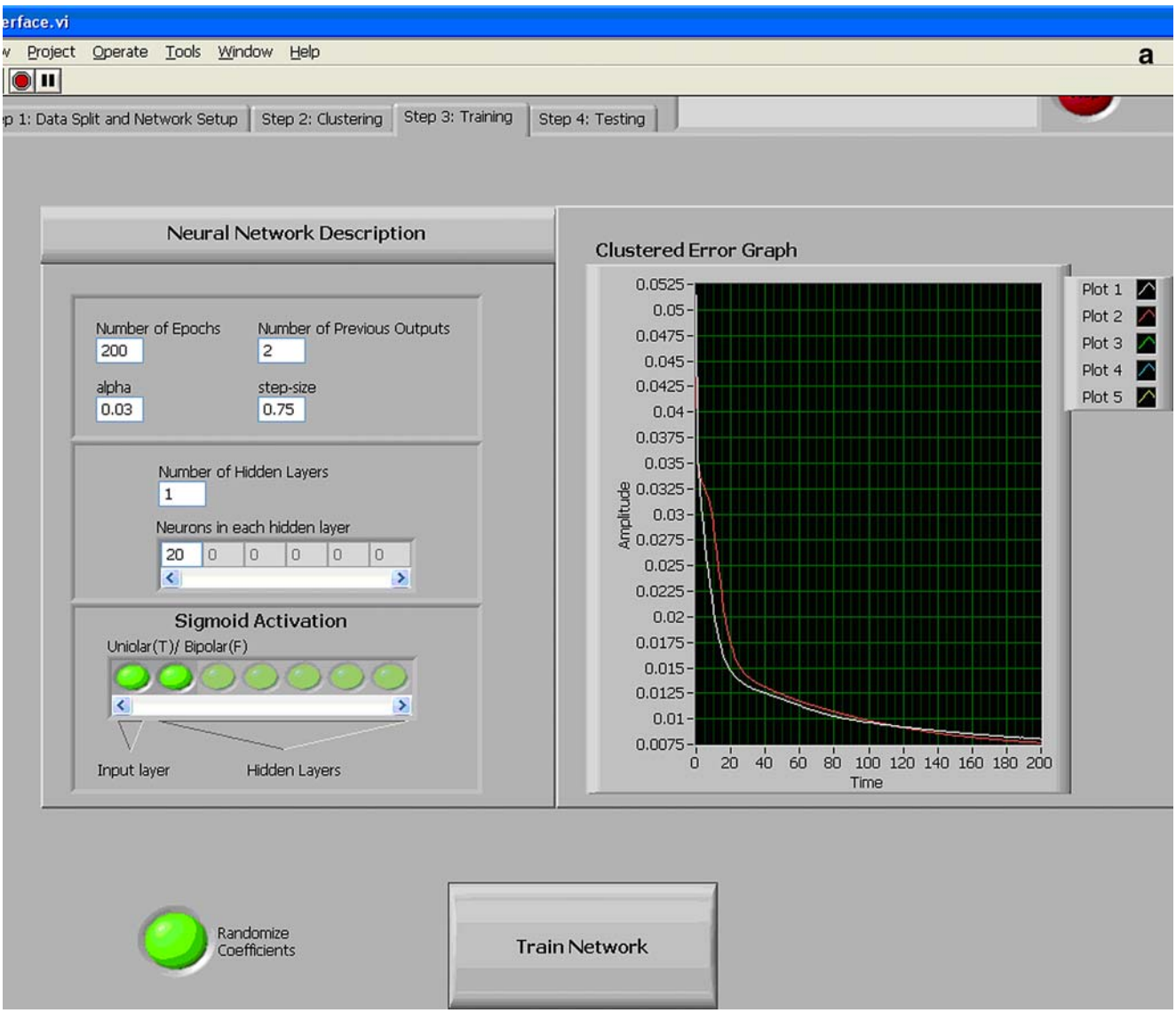

Fig. 8 **a** Training screen with the error at the end of the iterations. **b** Comparison between the ANN predictions with a randomly picked data for two different clusters

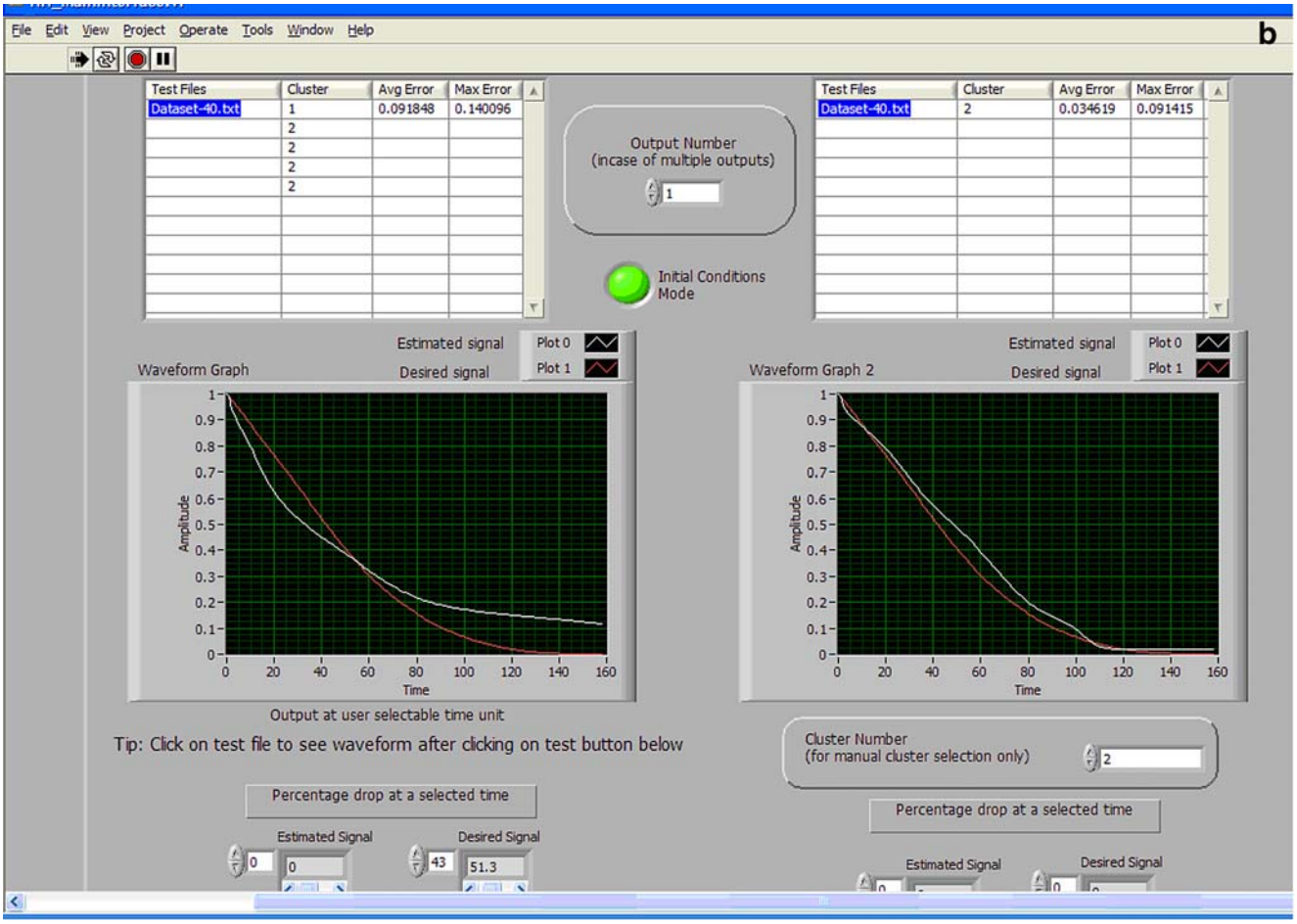

Fig. 8 (continued)

which is well under 1%. This analysis was done with two clusters. The program can have a maximum of seven clusters depending on the spread of data points. For instance, for higher temperatures, the evaporation rate increases significantly, and the prediction of a scenario at high temperature by the ANN will give better results if it is predicted with a particular cluster trained for this "high" temperature region.

A sample comparison is shown for the evaporation of HD on glass in Fig. 8b. The figure on the left shows the comparison with the first cluster, while the figure on the right shows a better result if the second cluster is used. The average error for the left figure is about 9%, and this is reduced to about 3.5% when the second cluster is used. Another advantage of the clustering option is to find "the best" match especially when a good resolution of data is not available. This is particularly the case when the agents are deposited on various porous substrates. Some agents may react with a substrate and produce more toxic chemicals. Therefore, in reality, the required number of data may not be available, and we have to do our best to determine "the best" possible prediction under all the existing constraints.

Conclusions

The neural network algorithms were successfully implemented to predict the output of two problems with a vector input. In the first application, the output was a scalar number, while in the second application, the output was represented by a function. In both cases, the neural network was utilized as a prediction tool based on a provided limited training set. The NN was also used to asymptotically lead us to the "minimum" number of required experiments needed from a large set that could reasonably represent the entire matrix. This approach has been shown to be particularly useful in creating a practical engineering tool for the outcome prediction of a large-scale problem. It should also be added that, in some cases similar to the second problem discussed in this paper, the cost of each test is currently about $15,000, and it is quite risky to work with hazardous materials. The ANN can be used to reduce this risk factor.

Acknowledgment This work has been supported in part by the Air Force Research Laboratory, Human Effectiveness Directorate, Bio-

sciences and Protection Division, Wright-Patterson AFB, OH, the Department of Energy, and the California Energy Commission (ECE).

References

Amin, M. (2006). Computational study on the effect of various parameters on the evolution of 2D free jet and its entrainment rates, Master thesis, The University of Washington, Seattle, USA.

Amin, M. Navaz, H., & Dabiri, D. (2008). Air curtain performance studies in open vertical refrigerated display cases. Proceeding of Heat Transfer 2008 Conf., 9-11 July, Slovenia.

Boyaci, I. K., Sumnu, G., Sakiyan, O. (2008). Estimation of dielectric properties of cakes based on porosity, moisture content, and formulations using statistical methods and artificial neural networks. Food and Bioprocess Technology, *1*(3). doi:10.1007/s11947-008-0064-z.

Cheng, B., & Titterington, D. M. (1994). Neural networks: A review from a statistical perspective. *Statistical Science*, *9*(1), 2–54. doi:10.1214/ss/1177010638.

Hajmeer, M-N., & Basheer, I-A. (2003). Review of microbiological modeling techniques for meat industry. *American Society of Agricultural and Biological Engineers*, ASABE Library.

Faramarzi, R., Amin, M., Navaz, H-K., Dabiri, D., Rauss, D., & Sarhadian, R. (2008). Air curtain stability and effectiveness in open vertical display cases. Final Report Prepared for the California Energy Commission, Public Interest Energy Research (PIER) Program.

Markicevic, B., Navaz, H. K. (2007). Primary and secondary spread of wetting droplet into porous medium. In: American Physical Society (APS), Division of Fluid Dynamics (DFD), 18-20 November 2007, Salt Lake City, Utah, USA.

Martins, R. C., Lopes, V. V., Vicente, A. A., & Teixeira, J. A. (2008). Computational shelf-life dating: Complex systems approaches to food quality and safety. *Food and Bioprocess Technology*, *1*(3), 207–222.

McCulloch, W. S., & Pitts, W. H. (1943). A logical calculus of the ideas immanent in nervous activity. *Bulletin of Mathematical Biophysics*, *5*, 115–133. doi:10.1007/BF02478259.

Navaz, H. K., Faramarzi, R., Dabiri, D., Gharib, M., & Modarress, D. (2002). The application of advanced methods in analyzing the performance of the air curtain in a refrigerated display case. *ASME Journal of Fluids Engineering*, *124*, 756–764.

Navaz, H. K., Henderson, B. S., Faramarzi, R., Pourmovahed, A., & Taugwalder, F. (2004). Jet entrainment rate in air curtain of open refrigerated display cases. *International Journal of Refrigeration*, *28*(2), 267–275.

Navaz, H. K., Amin, M., Dabiri, D., & Faramarzi, R. (2005). Past, Present, and Future Research Towards Air Curtain Performance Optimization. *ASHRAE Transactions*, *111*(Part 1), 1083–1088.

Navaz, H. K., Amin, M., Srinivasan, C. R., & Faramarzi, R. (2006a). Jet entrainment minimization in air curtain of open refrigerated display cases. *International Journal of Numerical Methods for Heat & Fluid Flow*, *16*(4), 417–430.

Navaz, H. K., Chan, E., & Kehtarnavaz, N. (2006b). A comprehensive study of HD sessile droplet evaporation on impermeable, non-reacting substrates. In: Chemical and Biological Defense Conference, November 2006, Hunt Valley, Maryland, USA.

Navaz, H. K., Faramarzi, R., & Amin, M. (2007a). CFD design of air curtain for open refrigerated display cases. In: Computational methods in food processing, pp129-141. CRC Press, Florida, USA.

Navaz, H. K., Chan, E., & Markicevic, B. (2007b). Convective evaporation model of sessile droplets in a turbulent flow—comparison with wind tunnel data. *International Journal of Thermal Sciences*, *47*, 963–971.

Navaz, H. K., Markicevic, B., Zand, A., Li, H., Chan, E., Sikorski, Y., et al. (2007c). The fate of the agent droplet deposited onto porous substrates—From modeling to operational field guide. In: Chemical and Biological Defense Conference (CBD), 13-16 November 2007, Timonium, Maryland, USA.

Navaz, H. K., Zand, A., Markicevic, B., Sikorski, Y., Sanders, M., & Chan, E. (2007d). Experimental and numerical study of evaporating droplet spread into porous substrate: Solution for (HD) and (VX) spread into UK Sand. DTRA (Defense Threat Reduction Agency). In: Workshop on Computational Chemistry, 13-17 August 2007, Maui, Hawaii, USA.

Patnaik, P-R. (2008). Intelligent models of the quantitative behavior of microbial systems. *Journal of Food and Biotechnology Technology.* doi:10.1007/s11947-008-0112-8.